Article

Preliminary Correlations for Remotely Piloted Aircraft Systems Sizing

**Álvaro Gómez-Rodríguez †, Alejandro Sanchez-Carmona †, Luis García-Hernández †
and Cristina Cuerno-Rejado †,*** ID

Department of Aircraft and Spacecraft, Escuela Técnica Superior de Ingeniería Aeronáutica y del Espacio, Universidad Politécnica de Madrid, Plaza del Cardenal Cisneros 3, 28040 Madrid, Spain; alvaro.gomez.rodriguez@alumnos.upm.es (A.G.-R.); alejandro.sanchezc@upm.es (A.S.-C.); luis.garcia.hernandez@alumnos.upm.es (L.G.-H.)

* Correspondence: cristina.cuerno@upm.es; Tel.: +34-913-36-63-65

† These authors contributed equally to this work.

Abstract: The field of Remotely Piloted Aircraft Systems (RPAS) is currently undergoing a noteworthy expansion. The diverse types of missions that these aircraft can accomplish, both in military and civil environments, have motivated an increase of interest in their study and applications. The methods chosen to develop this study are based on the statistical analysis of a database including numerous models of RPAS and the estimation of different correlations in order to develop a design method for rapid sizing of H-tail RPAS. Organizing the information of the database according to relevant characteristics, information relative to the state-of-the-art design tendencies can be extracted, which can serve to take decisions relative to the aerodynamic configuration or the power plant in the first phases of the design project. Furthermore, employing statistical correlations estimated from the database, a design method for rapid-sizing of H-tail RPAS has been conducted, which will be focused on the sizing of the wing and tail surfaces. The resulting method has been tested by applying it to an example case so as to validate the proposed procedure.

Keywords: remotely piloted aircraft systems; conceptual design; correlation analysis; RPAS database; RPAS design; H-tail RPAS

1. Introduction

Within the different sectors of the aerospace industry, Remotely Piloted Aircraft Systems (RPAS) presently stand out as one of the most dynamic. The origin of these aircraft date back to the beginning of manned aviation, having been employed for many decades as testing models and for military purposes, such as aerial targeting [1,2]. Recently, however, the integration of RPAS into an increasing range of civil-oriented missions and their further development in the military environment has heightened their impact in the aeronautical industry. The flexibility of these systems in developing a wide variety of missions has been noted, ranging from aerial photography to disaster relief [3], and their usage in specific missions that require an aircraft of small dimensions, that span an amount or time that would not be feasible to undertake for a single pilot, or a situation in the flight area that might pose a threat to a pilot on board has also been remarked upon [4,5]. Therefore, it is clear that the particular characteristics of RPAS compared to those of manned aircraft have established a new array of possibilities in aircraft missions, design, and planning.

The acknowledgement of the possibilities that RPAS present has motivated an increase in the resources dedicated to this area, especially from the year 2001 onward [6]. Furthermore, it is expected that the investment in RPAS will continue to increase in the near future. Precisely, multiple companies, universities, and research organizations have raised their interest in this field, which has led to

a significant increase in the number of RPAS projects in the last two decades. Commercial RPAS for civil operations are expected to experience the most notable growth, possibly expanding the number of RPAS of this type up to 10 times in the next five years in the US [7], where the most extended application is aerial photography, and it has been predicted that the growth rate will continue to accelerate in further years. Other studies point out that RPAS above 150 kg of Maximum Take-Off Weight (MTOW) are to be the most dynamic sector in the near future [3]. Regulatory institutions have taken part in the expansion of RPAS through rulemaking and the assignation of responsibilities, and the International Civil Aviation Organization has also considered these aircraft in the development of a global regulatory framework and providing guidance for national regulations [8,9].

The variety of environments in which these aircraft operate and the different types of missions for which RPAS are being developed have led to a significant variety in their design, as can be observed in the multiple tail configurations that have been tested, ranging from conventional tail configurations similar to those frequently seen in airliners, such as the T-tail, to more atypical ones such as the V-tail and H-tail. This diversity is also observed in the different payloads found on board, the variety of propulsion systems equipped and the launch and recovery systems implicated in their take-off and landing operations. In this context, the study of design tendencies for these aircraft and the development of rapid-sizing methods could benefit the further development of this field of aeronautics. Conceptual and preliminary design approaches to aircraft sizing have been developed by numerous authors in the field of transport aircraft [10–12], many of them being based on a statistical analysis on information of compiled aircraft in order to establish correlations amongst aircraft parameters. In recent years, these methods have been expanded on [13–15], even focusing on the optimization of certain aspects of the aircraft which had not yet been studied in detail and non-conventional tail configurations [16].

Despite the significant improvements upon conceptual and preliminary design methods in transport aircraft over the years, there is still room for improvement in regard to rapid-sizing tools for RPAS. Even though remotely piloted aircraft share their origins with aircraft in which the pilot is found on board, the surge in the research and development of RPAS, most significantly for those destined to civil purposes, is relatively recent. In the case of RPAS with high values of MTOW, their comparatively larger similarity with manned aircraft could allow the aforementioned conceptual design methods for traditional aircraft to be employed. However, for lightweight and middleweight RPAS, the differences with traditional manned aircraft become more notable, and the applicability of these design processes is not as evident. The result is that there are still no established rapid-sizing methods based on statistical correlations for the design of lightweight and middleweight RPAS. As remarked in other works pertaining the design of these aircraft, in some cases, the difficulty to gather information on design parameters can be due to the novelty of the program or the privacy of the project, which can make the compilation of a high-fidelity database a difficult task. Even if that information were available, the significant variety in RPAS configurations and designs constitute an added difficulty in estimating precise correlations, since the data tend to show a significant scatter due to the disparity amongst airframes, engine types, and missions [17]. Therefore, most times the design of RPAS is undertaken through constraint analysis and by fixing critical design parameters relative to those of similar aircraft [18]. Other approaches complement the classic conceptual design theory with optimization algorithms that estimate the design parameters by minimizing an objective function, which will depend on the characteristics and needs of the mission seeking to be accomplished [19].

The present paper revises the main design tendencies in the state-of-the-art for mini RPAS and includes a study based on correlations for developing a rapid design method for future aircraft in this category. The data and tools that have been employed to fulfil these objectives will be discussed in the Materials and Methods section. The first step has been to compile an extensive database of RPAS, attending to numerous design parameters, which will mainly focus on those that define the main aerodynamic surfaces: wing, horizontal tail-plane (HTP), and vertical tail-plane (VTP). In the case of certain aircraft configurations, these two last surfaces can be substituted with a V-tail, in which

further parameters will also be taken into consideration. The exposition of the information and conceptual design tools that have been extracted from the classification and analysis of these materials is conducted in the Results and Discussion section, of which the first point consists in the study of general design tendencies. These would be, for instance, the type of engine most commonly equipped to aircraft in a certain weight interval, as such data could assist in the conceptual design phase of an RPAS, in which multiple configurations are taken into account before selecting one of them to proceed to further phases of the project. One of the key aspects of these results is that a categorization related to MTOW has been set according to the limits established by many regulation Authorities. This will provide the designer information on the most common tendencies regarding aerodynamic configuration and power plant selection in each weight category. Taking into account regulation weight limits, which can have a notable impact in the certification requisites and costs, constitutes one of the novel aspects of the paper. Furthermore, for those RPAS categories for which the acquired data presents a significant fidelity and a number of aircraft that could permit the establishment of statistical correlations, the development of a rapid-sizing method will be expanded on. The resulting design method will then be applied to an example case not included in the database in order to verify the accuracy of the proposed design process.

The development of a rapid-sizing tool developed and tested specifically for RPAS constitutes one of the main contributions of the paper. The fast growth of the RPAS sector calls for the development of such conceptual design methodologies, which could aid the manufacturers to establish a favorable position in a very dynamic and demanding market. This methodology also includes in the estimated correlations aircraft with low values of MTOW that would not be feasible in manned aircraft and as such were not addressed in previous conceptual design procedures.

2. Materials and Methods

In order to study rapid-sizing methods for RPAS that are the purpose of this paper, the first step, in the same way as numerous authors that have developed conceptual and preliminary design tools based on statistical data correlations [10–12], which is to compile a complete and extensive database of aircraft. The information can then be studied in order to extract general design guidelines for RPAS, and, in the case of aircraft categories for which there is sufficient information, a design method based in correlations can be developed. A hypothesis that has been considered when compiling the information of the database has been only to include aircraft that develop conventional missions. Therefore, the unconventional cases would fall out of the scope of this paper.

Regarding the sources consulted in order to compile the parameters which have been included in the database, most of the data of the aircraft has been incorporated from information provided by the manufacturers, measurements in three view drawings and data found in the open literature [4].

The database consists of 398 aircraft. In spite of the number of RPAS present in the investigation, it should be noted that the information, which has been collected for most of them, has not been sufficient to guarantee the development of a correlation based design method for every category, since the process of data acquisition presents a variety of challenges [17]. The novelty of many of the civil RPAS projects and, in some cases, the difficulty to gather information relative to military aircraft due to the privacy of the project have had an effect on the volume of information that could be incorporated in the database. Furthermore, most of the parameters relative to tail surfaces, such as their span and surface, are not listed in the open literature and can only be obtained through measurement in three-view drawings of the aircraft. This is the reason for which, when estimating correlations that involve these parameters, the sample of aircraft available is not as exhaustive, since their values are only known for some of the RPAS. However, the procedure of measuring in three-view drawings has the advantage that it allows to assure that the same measuring criteria is used in all aircraft, which aids in the accuracy of the correlations estimated from the database.

The parameters that have been selected for the database compilation are mostly geometric and have been sorted into the following groups: general parameters, wing parameters, horizontal tail-plane

(HTP) parameters, vertical tail-plane (VTP) parameters, and V-tail parameters. These are the categories and the parameters that have been selected in each of them will be expanded upon.

2.1. General Parameters

This category includes weight parameters such as the aircraft Maximum Take-Off Weight (MTOW), Operating Empty Weight (OEW), and Payload Weight (PL). In particular, the MTOW parameter proves invaluable in that it is related to various aspects of the aircraft such as systems, payload, and mission and when deciding on a classification of the aircraft included in the database. The category also encompasses the general dimensions of the aircraft, in the form of span (b), length (l), and height (h), and it also incorporates the dimensions of the fuselage—length (l_f), width (w_f), and height (h_f)—which are directly related to the characteristics of the payload and the equipment on board. Being the element in the system that carries out the mission, and due to the diversity of missions that these aircraft develop, there is also an ample range of different payloads with varying characteristics, and as such, the fuselage design must be adapted to each particular case, resulting in varying fuselage dispositions and forms.

Finally, two parameters related to the aircraft performance, the cruise speed (V_c) and the endurance (E), have also been selected. The later parameter allows for a classification of the aircraft that will be crucial in determining the value of certain wing parameter in the design process.

2.2. Wing Parameters

The geometric parameters considered for the study of the wing surface are the following: wing span (b_w), root chord (cr_w), tip chord (ct_w), mean geometric chord (MGC_w), mean aerodynamic chord (MAC_w), wing surface (S_w), and quarter-chord line sweep ($\Lambda_{w1/4}$). These parameters allow us to obtain others that are dimensionless and of great value in aircraft design, precisely the Aspect Ratio (AR_w) and taper ratio (λ_w). These data will also permit the definition of further dimensionless parameters for the tail surfaces, which will be defined in the sections dedicated to the tail-planes. Another ratio, albeit dimensional, that has also been taken into account is the Span Loading (SL_w), which is defined as the ratio between the value of MTOW and the wingspan (b_w).

Upon observing the wing design of numerous RPAS, especially those of lower MTOW, it is evident that their wing planform present a high diversity. Most of them are designed with up to four sections with different taper ratios and sweep angles. This can greatly hinder the possibilities of obtaining relevant correlations for the wing parameters due to the inhomogeneity of the wing forms which are being compared, which could augment the scatter in the regressions. In order to solve this issue, an equivalent wing has been defined for each of the RPAS, based on the definition presented in previous works [11,20]. The properties of this wing are the following: the surface (S_w), span (b_w), and MAC_w are fixed to be the same as those of the original wing, and it will be composed of only one trapezial section, the sweep angle of which is computed as the average of the sweep angles of each section weighted with the span of each of them. This allows for a common wing definition that will allow for obtaining better results in the estimation of statistical correlations.

An additional parameter for the wing design has also been considered, which has its base in the definition of the induced drag coefficient considered in previous works [21], as shown in Equation (1).

$$C_{Di} = \frac{C_L{}^2}{\pi AR_w \varphi}.$$
(1)

To obtain this parameter, the previous equation can be expressed dimensionally. When combined with the vertical forces equilibrium equation that allows us to incorporate the weight of the aircraft in the expression, a relation between the induced drag and MTOW can be obtained, as seen in Equation (2).

$$Di = \frac{MTOW^2}{\frac{1}{2}\rho V^2 S_w \pi AR_w \varphi} = \frac{MTOW^2}{\frac{1}{2}\rho V^2 \pi \varphi b_w{}^2}.$$
(2)

2.3. Horizontal Tail-Plane (HTP) Parameters

Regarding the HTP, the geometric parameters which have been selected are equivalent to those chosen for the study of the wing. This includes the following geometric parameters: span (b_h), root chord (cr_h), tip chord (ct_h), mean geometric chord (MGC_h), mean aerodynamic chord (MAC_h), surface (S_h), quarter-chord line sweep ($\Lambda_{h1/4}$), and moment arm (l_h). The following dimensionless parameters have been considered: Aspect Ratio (AR_h), taper ratio (λ_h), and volume coefficient (V_h), which is expressed in Equation (3).

$$V_h \;=\; \frac{S_h l_h}{S_w MAC_w}. \tag{3}$$

2.4. Vertical Tail-Plane (VTP) Parameters

In the case of the VTP, the geometric parameters considered are also equivalent to those of the wing. The following geometric parameters have been studied: span (b_v), root chord (cr_v), tip chord (ct_v), mean geometric chord (MGC_v), mean aerodynamic chord (MAC_v), surface (S_v), quarter-chord line sweep ($\Lambda_{v1/4}$), and moment arm (l_v). The dimensionless parameters that complete the category are Aspect Ratio (AR_v), taper ratio (λ_v), and volume coefficient (V_v), which in this case is defined according to the expression shown in Equation (4).

$$Vv \;=\; \frac{S_v l_v}{S_w b_w}. \tag{4}$$

Additionally, since the vertical tail-planes observed in certain categories of RPAS present a significant diversity in their planforms, as was also observed in the case of the wing design, a similar procedure of defining an equivalent VTP is proposed. This equivalent surface has the same values for the parameters of surface (S_v), span (b_v), and, in this case, l_v, as the original VTP. In the case of the VTP, the moment arm was selected instead of the MAC_v since the former is more relevant in that it determines the relative position of the tail through the moment arm (l_v) and the volume coefficient (V_v), and thus the criteria were chosen so that these two parameters remain the same, so as to not disrupt the original tail arrangement. By defining this equivalent VTP for the aircraft in the database, it is expected that the correlations involving the design of these aerodynamic surfaces will present less scatter, as the planforms that will be compared will present a significant similarity amongst them.

2.5. V-Tail Parameters

The V-tail configuration is characterized by practically the same parameters as the HTP. However, since the aerodynamic surfaces have a considerable dihedral angle (Γ_{vee}) with the horizontal plane, a different category is considered for this configuration, since it most often replaces both the HTP and VTP, developing the functions of those surfaces simultaneously. Therefore, the same parameters as those of the HTP have been considered along with the dihedral angle (Γ_{vee}), separating those measured in the projection of the area in the horizontal plane, designated as "projected" values, and those in the non-projected surface, which have been referred to as "real" values.

2.6. Aircraft Classification

Having selected the parameters that will be taken into account in the study, the next step involves classifying the information in the database. The correct separation of the aircraft in different categories can prove crucial to obtaining adequate results when estimating correlations, especially since different RPAS designs present a high level of diversity, as has been previously noted. Most authors recommend a classification according to mission, altitude of operation, weight, or combinations of these criteria [2,4,20,22]. The mission that the aircraft will develop defines the type of payload it will carry and will therefore be critical in the fuselage design and in obtaining the MTOW. Even though a detailed analysis regarding the effects of the shape of the fuselage in the tail surface dimensioning

has not been conducted, it has been observed that the aircraft that fall in the category of H-tail RPAS present reasonably similar fuselage shapes. Since the rapid-sizing method based in correlations has been conducted for this category, it is expected that the correlations that estimate the parameters of the stabilizers will result in surfaces that take these effects into account, assuming that the fuselage of the design aircraft is similar to those of the database RPAS. Due to the difficulties commented beforehand on the design of RPAS, other works have also focused on specific elements of the aircraft, such as the fuselage design [17].

Therefore, the main organization of the aircraft has been set according to the aerodynamic configuration. This is the categorization that yields the best results when sorting the RPAS in the database for obtaining the statistical correlations that will be further expanded upon in this work, since it determines the relative position amongst the aerodynamic surfaces and groups those aircraft that present similar arrangements, reducing the scatter of the data in the correlations. The groups which have been considered are the following: conventional tail, T-tail, V-tail, Y-tail, H-tail, delta wing, no HTP, tailless, canard, joined wing, ring tail, cruciform tail, and tandem wing. Since in some cases the tail configurations can present particularities, and in order to provide an example on the aircraft classification criteria, Figure 1 includes various RPAS and the category in which they have been included.
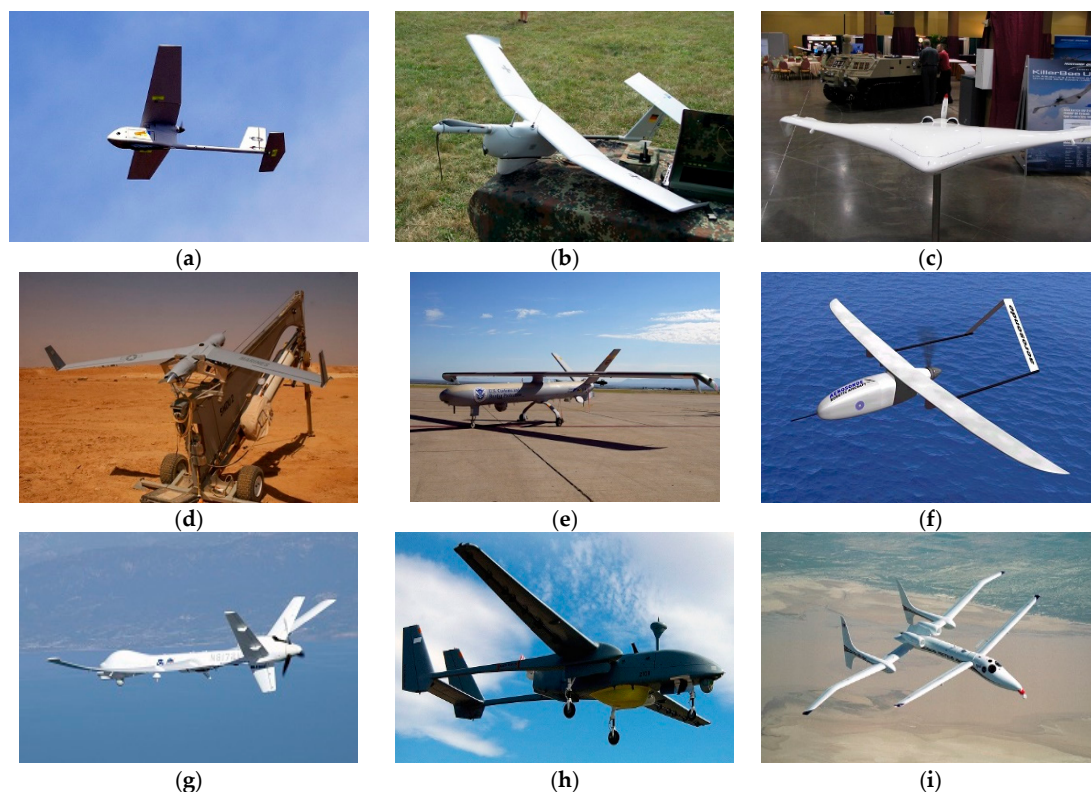

Figure 1. Examples of Remotely Piloted Aircraft Systems (RPAS) that have been considered in the different aerodynamic configuration categories (images from https://commons.wikimedia.org). (**a**) AeroVironment RQ-11 Raven, conventional tail RPAS; (**b**) EMT Aladin, T-tail RPAS; (**c**) Northrop Grumman KillerBee, tailless RPAS; (**d**) Boeing Insitu ScanEagle, also considered in the tailless category; (**e**) Elbit Hermes 450, V-tail RPAS; (**f**) AAI Aerosonde, V-tail RPAS; (**g**) General Atomics Altair, Y-tail RPAS; (**h**) IAI Heron, H-tail RPAS; (**i**) Scaled Composites Proteus, included in the tandem wing category.

As it can be seen, even after classifying the RPAS in different groups, there are still geometries present in the same categories which are considerably different. This seems especially evident in the cases of the tailless category and the V-tail category, as deduced from Figure 1. Every category presents

differences amongst the different RPAS included in them, such as the use of tail booms or the design of the fuselage. It is expected that those aerodynamic configurations which are more homogenous will be more viable for the development of a rapid-sizing method based on correlations. Nevertheless, in the case that different tendencies are observed within the same category, different sub categories can be proposed in order to further group the aircraft.

Other categorizations that have been considered to sort the information in the database have been the type of engine (electric motor, piston engine, turbo engine, and no engine), the launch system (conventional runway take-off and assisted launch), and finally a classification regarding the value of MTOW, for which four ranges have been considered: up to 25 kg, from 25 kg up to 150 kg, from 150 kg up to 1000 kg, and more than 1000 kg. The limits of each of these categories have been chosen following the limits which are most commonly observed in different regulations. For instance, in the case of US regulations, RPAS under 25 kg of MTOW operated in specific conditions are regulated according to Part 107 of the Title 14 of the Code of Federal Regulations [23], whereas different rules apply to RPAS with a value of MTOW above that threshold. In the case of European regulations, RPAS above 150 kg of MTOW are regulated by the European Aviation Safety Agency (EASA, Cologne, Germany), whereas those below this value fall within the competence of the European Union (EU, Brussels, Belgium) Member States (MSs), albeit this situation could change in the near future through a new regulatory framework being developed by the EU that would make all RPAS to be under the regulation of the Agency [24]. Nevertheless, in this work, these ranges can provide an insight on the weight distribution of RPAS that can be observed in the aircraft included in the database. This classification can be related to the complexity of the system, the size of the aircraft, and also to the kinetic energy of the system, which can correlate with the damage associated with the impact of the aircraft. This has been considered as one of the criteria that regulations have employed to set the different weight limits for the establishment of a regulatory classification [25]. The number of engines, being a classification that usually yields good results in transport aircraft [16], cannot be applied in this case, since nearly all of the aircraft considered present a single engine.

Finally, regarding the development of a rapid sizing tool for RPAS, the method that has been selected for this purpose has been the estimation of statistical correlations from the parameters included in the database. This procedure is expected to fit with the needs of the conceptual design phase, in which the acceptable error should be lower than 10%, and the focus is set on providing an initial approach for the design parameters of the aircraft with rapid methods. Furthermore, it should be noted that the regressions that have been estimated in this manuscript have been selected based on relevant design parameters such as the wing loading (W/S_w), the span loading (W/b_w), and the volume coefficients (V_h, V_v). Therefore, when estimating a correlation, the underlying physics that justify the relations amongst the design parameters have been clarified.

3. Results and Discussion

The results and conclusions obtained upon completing the database and categorizing the information can be divided in two parts: in the first one, regarding the study of design tendencies, the process that has been followed has been to classify the information according to various relevant aspects of design that were exposed in the end of the previous section, and then checking which categorizations are more extended in the state-of-the-art of RPAS. This information can serve as basis for the conceptual design phase of a project, in which several configurations and options are being considered as potential designs, as having some design guidelines can assist in this process. In the second part, for the category of H-tail RPAS, in which the sample of aircraft can guarantee a high level of fidelity, a conceptual design approach of rapid sizing has been proposed.

3.1. General Design Tendencies

Attending to the categories which have been used to organize the information present in the database, the RPAS have been sorted attending to these criteria. Table 1 illustrates the number of aircraft in each category when organized by aerodynamic configuration and MTOW range.

Table 1. Database RPAS classification attending to aerodynamic configuration and weight.

MTOW (kg)	<25	[25,150)	[150,1000)	>1000	Unknown	Total
Conventional tail	45	18	5	3	3	74
T-tail	30	18	7	5	0	60
Wing and VTP	12	0	1	0	0	13
Delta wing	2	2	1	0	0	5
Tailless	27	4	1	6	0	38
Joined wing	3	0	0	1	1	5
V-tail	29	16	15	12	1	73
Y-tail	1	2	0	6	1	10
H-tail	9	39	37	14	2	101
Canard	1	2	4	0	0	7
Tandem wing	2	0	0	2	0	4
Ring tail	0	1	0	0	0	1
Cruciform tail	0	0	1	0	0	1
Unknown	1	2	1	0	2	6
TOTAL	162	104	73	49	10	398

The first conclusion that can be obtained from this information is the identification of those categories for which the development of a design method based on statistical correlations can be feasible. The categories of conventional tail, T-tail, V-tail, H-tail, and tailless are the ones for which more information is available, which in turn signifies that a larger sample for the statistical study is available. Therefore, these groups will be considered in the second section of the discussion for the analysis of possible rapid-sizing methods. Another significant conclusion that can be deduced from these numbers is that these are the most commonly used aerodynamic configurations for RPAS design, whereas the rest of configurations considered serve more particular purposes and have not yet been expanded upon as much in this field. Regarding the MTOW, it is also noteworthy that most of the models included in the database could be classified as lightweight and middleweight RPAS. This is coherent in the sense that most of the missions conducted by these aircraft can be carried out with light payloads, and a result, the overall weight of the aircraft is relatively low. Additionally, many RPAS projects tend to exploit the characteristic of having a remote pilot and carrying no passengers, and a result the equipment related to cabin conditioning and evacuation systems, amongst others, can be neglected, resulting in aircraft with lower weight than that which would be feasible with humans on board. The further study of this category of RPAS could prove valuable, since it has been noted that studies conducted in the US show that the sector of RPAS below 25 kg of MTOW is very dynamic and their growth is expected to accelerate over the next few years [7]. In fact, it has been noted that many of the small RPAS designs correspond to the first projects of small and medium enterprises which are starting their development in the civilian RPAS market [25].

Attending to the cross-examination of the information regarding the MTOW range and aerodynamic configuration provided by the table, it is possible to extract several conclusions on the design tendencies of RPAS. As can be seen, the configurations of conventional tail and T-tail are employed in a notable number of lightweight RPAS, but in turn, they are less frequently used for heavier aircraft. The extended use of the T-tail is of special interest, since it tends to be used in aircraft with twin engines attached to the rear fuselage. This situation, however, is not applicable in most RPAS, since the vast majority of these aircraft have only a single engine. Even so, this tail configuration

is relatively common in lightweight RPAS. This may be due to the recovery of most of these aircraft consisting in a belly landing or deep stall maneuver, which are feasible in this kind of RPAS.

In the case of higher-weight aircraft, these configurations are not employed as often compared to the V-tail and H-tail configurations. In the case of the T-tail configuration, the belly landing is no longer feasible due to the high weight of the aircraft, nor is the aforementioned engine integration possible, as these RPAS still carry in most cases only one engine. The main advantages it presents cannot be taken advantage of, and so other tail configurations are selected above this one. Engine integration could be one of the main reasons for this choice, since, having a single engine, the frontal tractor position could potentially interfere with the payload, whereas its integration in the tail cone could prove difficult due to the presence of the tail structure. In the case of the H-tail configuration, this problem is solved through the use of tail booms, which allow the positioning of the tail surfaces after the end of the fuselage. Also, in certain scenarios of V-tail RPAS, the space between both tail surfaces allows for a relatively direct integration of a turbo engine. It should also be taken into account that the preference for other tail layouts could be due to the fact that they have already been employed in similar RPAS and are preferred by the manufacturers due to the experience they have already gained working with these configurations in previous projects.

Following on the discussion developed in the previous paragraph, the V-tail and H-tail also show a significant use in RPAS. It is noteworthy to check that the V-tail configuration is commonly employed in all MTOW range categories. However, H-tails tend to be used in the higher MTOW ranges. As stated in the work of previous authors [12], the objective of the V-tail is to reduce the wetted area, and with this, the aerodynamic drag. This tail encompasses the missions of both traditional HTP and VTP surfaces simultaneously, which also implies that the complexity of control is increased. This is the reason for the problem of adverse coupling between yaw and roll due to the deflection of the tail control surfaces that occurs in this configuration [12].

The higher level of aerodynamic and structural complexity that this configuration involves may explain why it is not used as often in lightweight RPAS compared to conventional and T-tail configurations, even though it still represents a significant category within the study population. In the case of aircraft that land with a belly landing maneuver, this configuration proves advantageous, as in the case of the T-tail, since the dihedral angle would prevent a collision of the aerodynamic surfaces with the ground in the case that a roll perturbation occurs. It is feasible to deduce that this may be the reason for the notable use of this configuration in small RPAS, even though the conventional and T-tail layouts are preferred. It is also significant to note that many V-tail configurations also employ tail booms in which the rear aerodynamic surfaces are located, instead of being joined directly to the fuselage. The reasons behind this preference are discussed in the following paragraphs along with the H-tail.

The frequent use of the H-tail, which in most cases also involves tail booms, in these aircraft is also remarkable. The use of various vertical tail surfaces is common in those cases in which the dimensions of a single vertical tail-plane could be considered excessive, especially in terms of the aircraft fitting in certain spaces such as hangars. This motivation is meaningful in the field of RPAS, as many of them are usually transported in vehicles that also serve the purpose of Ground Control Systems (GCS). This means that the capacity to fit the aircraft into a movable container is vital in order to deploy the RPA where the mission will take place, hence the importance of reducing the dimensions of the aircraft. On the other hand, the H-tail usually is heavier than the equivalent single VTP tail. This may explain why, contrary to the V-tail case, this configuration is reserved for heavier aircraft, as in smaller RPAS, the weight addition and more complex design of this tail compared to a simpler conventional tail cannot justify its selection. Opposite to this scenario, in heavier aircraft, the weight difference is not significant, and the dimensions can start restricting the transportation, therefore opting for the H-tail.

Regarding the use of tail booms, several RPAS designs employ them in order to connect the tail surfaces with the rest of the aircraft rather than joining them directly to the fuselage. The reason for their relatively frequent use in RPAS could be due to the characteristics of the payloads employed for

the variety of missions that these aircraft develop. It can be assumed that most times, the payload along with the fuel can fit in a relatively modest fuselage. However, the tail surfaces still need to be located at a certain distance of the center of gravity in order to provide the necessary aerodynamic moment for the stabilization and control of the aircraft. Instead of extending the fuselage, which is not usually needed since the equipment and fuel fits in a shorter cabin, and as it would add both additional weight and wet surface, the latter of which results in increased drag, tail booms are fitted in the wing or the fuselage, which extend further from the end of the fuselage in order to position the tail surfaces. Additionally, if the presence of a camera or other payload in the front fuselage is being considered in the design, which is also common in RPAS, as there is usually a need of a camera in order to monitor the aircraft operation, the propeller preferably installed in the rear of the aircraft. This provides a good fit for the mentioned configuration, as the propeller can energize the aerodynamic flow, producing a increase in the dynamic pressure on the tail-planes and allowing to obtain higher aerodynamic forces with the same surface than a tail that does not benefit from this effect [26]. Furthermore, recalling the engine integration discussion, the use of tail booms allows for more volume of the rear fuselage to be available for housing the engine and propeller than a conventional union of the tail surfaces to the fuselage. Another effect that the propeller has in this position is the reduction of base drag caused by the fuselage end.

The relatively frequent use of the tailless configuration in RPAS should also be expanded upon. However, this categorization is not quite as homogeneous as the others, as there are different design approaches that have been included in this category, from all-wing configurations without a defined fuselage to hybrid flying wings, including intermediate blended-wing-body models. Most of the drawbacks that this configuration present in manned passenger aircraft, such as those relative to evacuation, high angle of attack of the aircraft, and pressurization, are irrelevant in a remotely piloted aircraft that does not carry humans on board [27]. The capacity to avoid these negative aspects, along with the advantages of this layout, such as lower wet surface that in turn results in drag reduction, can explain the frequent use of this configuration in RPAS, which can be observed is more extended in the case of low weight aircraft.

Other aerodynamic configurations have also been tested in RPAS. However, as can be seen in the table, they have not yet benefited from frequent use and are mostly related to experimental projects and particular cases.

Table 2 presents the number of aircraft sorted both by MTOW and engine type.

Table 2. Database RPAS classification attending to engine and weight.

MTOW (kg)	<25	[25,150)	[150,1000)	>1000	Unknown	Total
Electric motor	132	6	0	0	3	141
Piston engine	30	91	69	27	3	220
Turbo engine	0	2	0	22	0	24
No engine	0	0	1	0	0	1
Unknown	0	5	3	0	4	12
TOTAL	162	104	73	49	10	398

Table 2, along with Table 1, could allow us to, in the case the value of MTOW is known, select the most common engine type and aerodynamic configuration for the early design phases of the RPAS. In the case of the engine type, electric motors dominate the category of low weight aircraft. This is due to the ease of acquisition of small brushless motors, which are in most cases the type of power plant employed to drive the propellers of small RPAS, since the level of thrust required by these aircraft is appreciatively lower than that of heavier aircraft. This can be deduced from the horizontal equilibrium equation in cruise flight, which relates the thrust provided by the engines with the drag of the aircraft, being the values of both forces comparable. The latter is expected to be lower in lighter RPAS due to them presenting a reduced airframe, and therefore the power output provided by electric

motors is enough to justify their selection. Even though these could also be equipped on large aircraft, the power demand would be higher due to the increased drag, and therefore, the batteries would need to have very high specific capacity in order to provide the necessary power output while not penalizing the weight of the aircraft. This is the reason for electric motors not being commonly used in larger aircraft. This relation amongst MTOW, thrust and drag will be further expanded on in the proposed rapid-sizing method. In contrast with the former arguments, the endurance that can be achieved with these power plants is in most cases much less than that which could be obtained with piston engines, these being more complex and costly than electric motors. Therefore, these small and light aircraft usually develop low endurance missions, and the capacity to change batteries, which are easily carried and swapped for others, allows the mission time to be extended. However, for heavier aircraft, they are impractical, since the weight and number of batteries needed to provide the necessary thrust becomes such that the designers opt for other alternatives. The few electric motors that can be observed in heavier aircraft actually correspond to solar powered RPAS. The investigation on long-endurance aircraft powered with solar energy is still ongoing, and they still constitute a minority amongst the other types.

Moving on to higher weight RPAS, it can be observed that the electric motors are replaced with piston engines. These are generally piston engines, with a variable number of cylinders, that move a propeller. However, rotary engines are also equipped in many RPAS, mainly those of higher weight. Piston engines usually allow for higher endurance missions and constitute the engine category most frequently used in RPAS, since the specific fuel consumption is usually lower than the discharge rate of Lithium-Polymer batteries often used in conjunction with electric motors, allowing for more operation time. Most of the missions that these aircraft carry out, such as surveillance or monitoring, do not require a cruise speed such that transonic effects appear at the tip of the propeller blades. Therefore, the combination of a piston engine and a propeller constitutes the most common selection, being coherent with the moderate endurance and cruise speed mission requisites.

Regarding the category of highest MTOW, both turbo engines and piston engines have been employed as propulsion systems. The use of turbo engines such as turbojets and turbofans in RPAS is reserved for the larger and heavier aircraft, usually military models which can fly at high speeds, even reaching values of Mach number (M) of M = 0.8, as these engines have a much more efficient performance at these flight speeds than propulsion systems based on propellers, save for turboprops, which have also been equipped on RPAS flying at speeds around M = 0.6. These were also included in the turbo engine category in Table 2. In the case of these military RPAS, cruise speed is most often crucial in the missions they carry out, and as such, a different alternative to the piston engine driving a propeller is required.

Therefore, it can be concluded that the value of MTOW can provide an early approximation to the type of engine which could be equipped on the aircraft, considering the mission speed to be expected depending on the mission in order to check the viability of the selected power plant.

3.2. Rapid-Design Method Based on Correlations for H-Tail RPAS

Having analyzed the characteristics of the resulting database, such as the number of aircraft in each category and the most relevant configurations in RPAS, the next step consists in the development of a rapid design method based in statistical correlations. Upon organizing the database and analyzing the results when establishing general correlations, it has been noted that the aerodynamic configuration is the characteristic that affects the most the results of the parameter dependency analysis. Therefore, the approach that has been considered in this study has been to segment the statistical population into different groups according to the aerodynamic configuration and to study the correlations separately for each of them.

Amongst the considered categories, the most relevant ones in the database, as noted formerly, are the following: conventional tail, T-tail, V-tail, H-tail, and tailless. The last of them, which encompasses all RPAS without a distinguishable tail, is not as homogeneous as the other categories, presenting a diversity

of fuselage-wing unions and very different wing planforms. Therefore, significant correlations between the parameters considered have not been obtained so far. The case of the V-tail configuration is similar, as even though it includes a greater number of aircraft, the considerable presence of this configuration in all ranges of MTOW, and the different forms in which to incorporate the V-tail consequently scatter these sub-categories in the dependency analysis. Different ways in which the V-tail can be observed include upward or downward V-tail joined to the fuselage, upward or downward V-tail with a tail boom, or a downward V-tail with twin booms. Regarding the conventional and T-tail configurations, the database would have to be expanded upon in order to facilitate obtaining accurate correlations, since for these categories, not many three-view drawings have been found, and as such, there is little information regarding the tail surfaces in the database so far, since the parameters relative to these surfaces are not usually found in the open literature, making it necessary to measure them in an adequate image.

This leaves the H-tail layout, which in turn presents a favorable set of characteristics regarding the study of a design method. The aircraft included in this category are more homogeneous than those of the other, consisting in a fuselage and twin booms to which the tail surfaces are attached. These consist of an HTP joined to both booms and twin vertical tail-planes usually found at the end of the horizontal tail-plane. The configuration is mostly used for higher MTOW aircraft, which are also more uniform than lightweight ones, and the type of engine equipped is predominantly the piston engine. Furthermore, many aircraft in the database are included in this category, so the sample of study is also sufficiently large.

Attending to these criteria, the H-tail configuration has been selected in order to develop a rapid design method for the first phases of the RPAS project. The objective is to design the main aerodynamic surfaces (wing, HTP, and VTP) employing statistical correlations obtained from the database. In most correlations, not as many points as aircraft contained in the group will be observed, since, as mentioned beforehand, specific parameters relative to the tail surfaces could not be obtained except through measurement in three-view drawings. Also, in the case where the measurement criteria employed by the source could not be checked, the data have been omitted, so as to reduce the scatter in the correlations. For instance, this occurs in the measuring of the wing surface (S_w), since depending on the source, the portion that is located inside the fuselage can be computed by different means. This decision has also lead to the presence of less aircraft in the correlations. However, it can be assumed that, by reassuring that the same criteria of measurement is used in all aircraft, the results can be more accurate. As will be seen in the correlations, most of the aircraft that have been analyzed are comprised in the range of 100 kg and 300 kg of MTOW, whereas two of the RPAS are located at higher MTOW values.

To start the design process, it is necessary to define which parameters can be considered design specifications. That is, this information constitutes the basis of the design and can be considered as an input in the process. These specifications will be MTOW, endurance, and the expected cruise speed (V_c), which will depend on the type of mission. The value of MTOW can be a significant design parameter due to the differences between the regulations applied to these aircraft depending on this characteristic, and it is also coherent with the categorization developed in the database analysis. The endurance and cruise speed are related to the mission that the aircraft has to accomplish, so it is also reasonable to set both as design parameters in order to guarantee that the RPAS can develop the mission for which it was designed.

From this point on, the different correlations which constitute the design process will be proposed and developed upon.

3.2.1. Wing Design

The first step of the design process consists in obtaining the value of the wing area, S_w. The correlation presented in Figure 2 establishes a relationship between the value of MTOW and S_w, which has been represented as a linear equation, such as those presented by other authors [13,16]. This correlation is based on the wing loading parameter, defined as the ratio between the value of

MTOW and the wing surface, which affects many design characteristics of the aircraft, such as the design point when compared to the thrust-weight ratio and the response to vertical gusts.
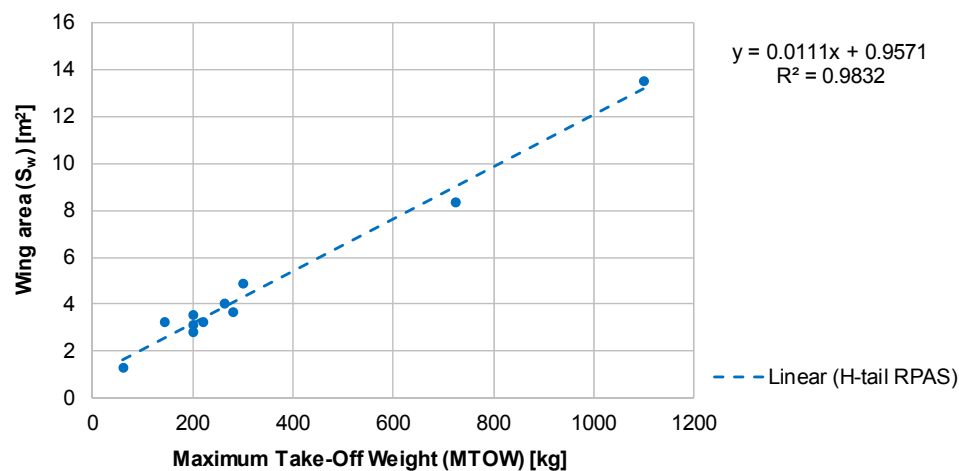

Figure 2. Wing area–Maximum Take-Off Weight correlation, with a typical error of 0.66 m^2.

In order to obtain the wingspan (b_w), the wing induced drag parameter, expressed previously in Equation (2), will be employed. In the aforementioned equation, it can be seen that the induced drag is in relation to the Aspect Ratio (AR_w) of the wing, and thus it is connected to the value of the wingspan (b_w). Wings with larger values of AR_w will have lower induced drag, which consequently benefits the flight endurance of the aircraft, as it will be reflected in the following regression. In order to connect this expression with the parameters that are known at this step of the design process, the value of the induced drag can be related to the weight of the aircraft, as reasonably, heavier RPAS are expected to present an increased drag resulting from a larger airframe. Therefore, this parameter links the value of MTOW to the wingspan, and so the correlation presented in Figure 3 has been built comparing the value of MTOW to the ratio between this weight and b_w. This correlation is similar to those employed in previous works to size the wingspan [21].
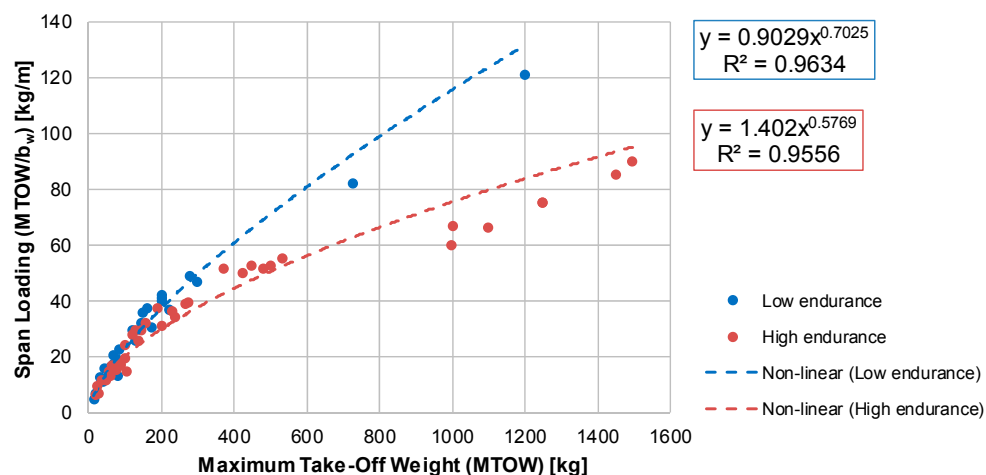

Figure 3. Span Loading–Maximum Take-Off Weight correlation, with a typical error for low endurance of 4.16 kg/m and a typical error for high endurance of 5.69 kg/m.

It can be seen that the aircraft follow two different tendencies, according to the endurance selected in the design specifications. Generally, aircraft with higher endurance present a lower induced drag ratio, since their wingspan is larger than those that have less endurance. This is coherent with the fact

that wings with larger Aspect Ratios have reduced values of the induced drag, as seen in Equation (2). In order to determine the group that the design aircraft belongs to, the reference presented in Table 3 can be consulted. This classification establishes an endurance threshold which, depending on the value of MTOW, determines whether an aircraft is to be included in the high endurance correlation or the low endurance one. This endurance threshold varies depending on the value of MTOW since larger aircraft have more fuel capacity, and therefore it is more feasible to obtain high values of endurance, even with larger values of induced drag due to low values of AR_w.

Table 3. RPAS classification attending to Maximum Take-Off Weight (MTOW) and Endurance in the induced drag parameter correlation.

MTOW (kg)	Endurance (h)	Classification
<150	≤ 4	Low endurance
	>4	High endurance
[150,200)	≤ 6	Low endurance
	>6	High endurance
[200,600)	≤ 10	Low endurance
	>10	High endurance
≥ 600	<20	Low endurance
	≥ 20	High endurance

Having obtained both S_w and b_w, in order to define the chord distribution of the wing, the value of the taper ratio (λ_w) must be estimated. It has been observed that the taper ratio of the RPAS object of this study present significant scatter, ranging from constant chord wings to highly tapered ones. However, when classifying the aircraft in four groups regarding different design and performance parameters that are related to the taper ratio, it can be observed that each of them contains RPAS with similar tapered wings.

The parameters that have been used to classify the aircraft in these groups are related to the characteristics influenced by the taper ratio. One of the main reasons for the addition of taper to wings is to avoid high bending root moments [10]. As was seen in the S_w–MTOW correlation, the value of MTOW can provide a general idea on the size of the wing, and therefore, the aerodynamic forces that will appear. This can explain why for high MTOW aircraft, wings tend to show significant taper. The Aspect Ratio and Span Loading parameters are both also related to this characteristic, since they also provide an idea on the dimensions of the wing, and more specifically, its span compared to the surface and the MTOW, respectively. Regarding the performance parameters, their selection was made as means of measuring the difference in induced drag that a tapered wing presents compared to an untapered one [12]. Therefore, it can be expected that tapered wings will have more endurance and higher cruise speeds precisely due to the drag reduction, since the lift distribution becomes more similar to an elliptical distribution, which is the lift distribution that provides a lower value of induced drag.

Therefore, the proposed method to estimate the wing taper ratio (λ_w) consists in taking into account the input value of the design process MTOW and considering the wing Aspect Ratio (AR_w) and the Span Loading parameter (SL_w), which was defined in the second section of this paper as the ratio between the value of MTOW and the wingspan (b_w). Furthermore, two performance parameters will also be taken into account: the cruise speed (V_c) and the endurance (E). The values of these parameters will determine in which category the design aircraft is included, following the flowchart present in Figure 4.
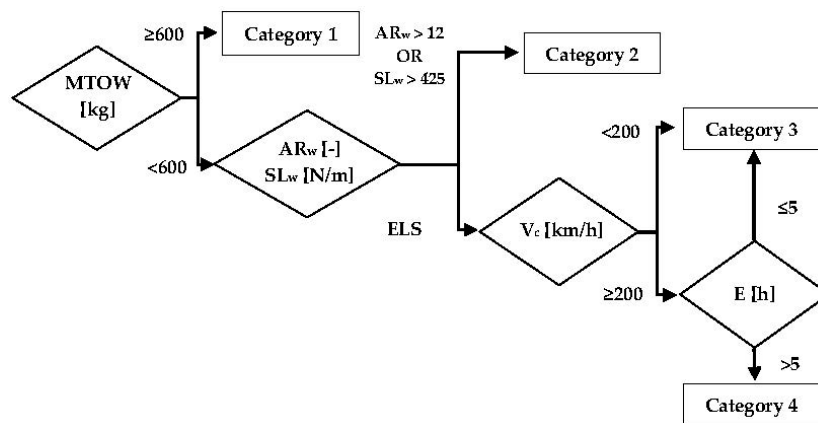
Figure 4. Flowchart for the categorization of RPAS in groups of similar wing taper.

Having selected in which group to include the design aircraft, Table 4 presents the designation of the different groups along with the estimated range of expected taper ratio and the mean values of this parameter within each category for the aircraft which have been studied. This would allow the designer to select a suitable value for this parameter so as to continue the design process.

Table 4. RPAS classification attending to taper ratio.

Category	λ_w Range	λ_w Mean
1	(0.50–0.65)	0.58
2	(0.40–0.60)	0.46
3	(0.85–1.00)	0.97
4	(0.60–0.86)	0.67

Having obtained the values of S_w, b_w, and λ_w, the values of the root chord, the tip chord, and the mean aerodynamic chord can be estimated through the following equations, which constitute the definitions for S_w, λ_w, and MAC_w, respectively:

$$S_w = \frac{cr_w + ct_w}{2} b_w, \tag{5}$$

$$\lambda_w = \frac{ct_w}{cr_w}, \tag{6}$$

$$MAC_w = \frac{2}{3} cr_w \frac{1 + \lambda_w + \lambda_w^2}{1 + \lambda_w}. \tag{7}$$

Solving the equation system (5–7) for cr_w, ct_w, and MAC_w, the chord distribution for a simple tapered wing has been defined. Should the designer prefer a wing divided in different sections, each of them having a different taper ratio, the equivalent wing definition proposed in the second section of this work can be used, in order to maintain a similar performance to the wing obtained throughout this process.

In particular, the value of MAC_w constitutes a crucial parameter in the definition of other parameters relative to the tail surfaces, such as the volume coefficients (V_h, V_v). In order to finalize the wing design, a value of wing sweep should be selected. Generally, RPAS travel at relatively low speeds, and the wing sweep is usually employed in order to increase the critical Mach (M_c) value for aircraft travelling at close to transonic speeds, so as to delay the appearance of transonic effects and shockwaves in the wing. This is not the common case for RPAS, so the values of wing sweep are usually low. In the aircraft object of this study, the value of quarter-chord sweep ($\Lambda_{w1/4}$) usually ranges from 0° to 5°.

3.2.2. HTP Design

In order to undertake the design of the horizontal tail, the first parameter which will be estimated, as in the case of the wing, is the surface (S_h). A correlation that compares the value of S_w with S_h is proposed, as the ratio between these two surfaces has been used in previous works as a mean of estimating a value for S_h [10]. As can be seen in Figure 5, the resulting correlation is linear and yields a relatively accurate result.
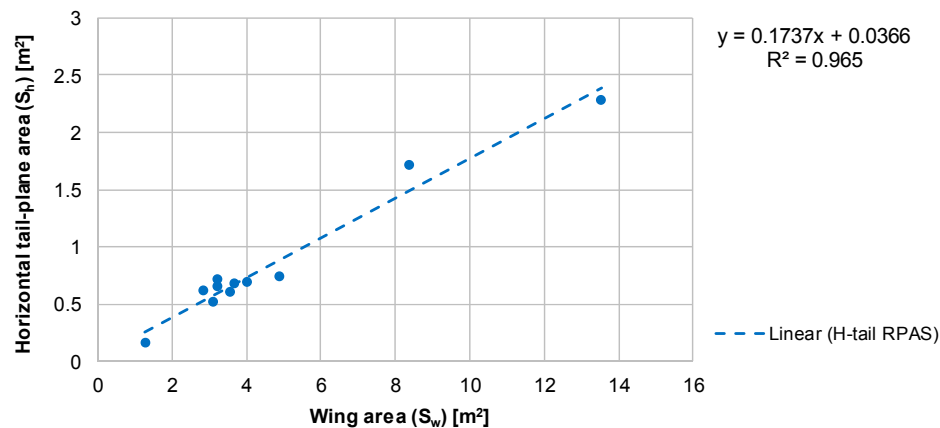

$$y = 0.1737x + 0.0366$$
$$R^2 = 0.965$$

Figure 5. Horizontal tail-plane area–Wing area correlation, with a typical error of 0.12 m^2.

Once the surface of the HTP has been estimated, the next step consists in locating the position of the horizontal tail-plane relative to the wing. This distance is measured through the moment arm parameter (l_h). In order to obtain this value, the correlation represented in Figure 6 resorts to the definition of the dimensionless HTP volume coefficient (V_h), which was previously expressed in Equation (3). The numerator of the volume coefficient ratio is compared to the denominator, thus entering the correlation with the values of S_w, MAC_w, and S_h, the moment arm (l_h) and the volume coefficient (V_h) can be obtained.

Regarding the planform of the HTP, it is noteworthy that all of the aircraft included in this category in the database present a rectangular planform for the horizontal tail-plane. Therefore, the HTP chord is constant and the sweep angle is zero. These guidelines are also taken into account in the design process. Therefore, once the wingspan of the HTP is defined, the chord can be estimated through the ratio between S_h and b_h, and thus the value of the chord is obtained, and as it is constant, it coincides with the values of MGC_h and MAC_h.
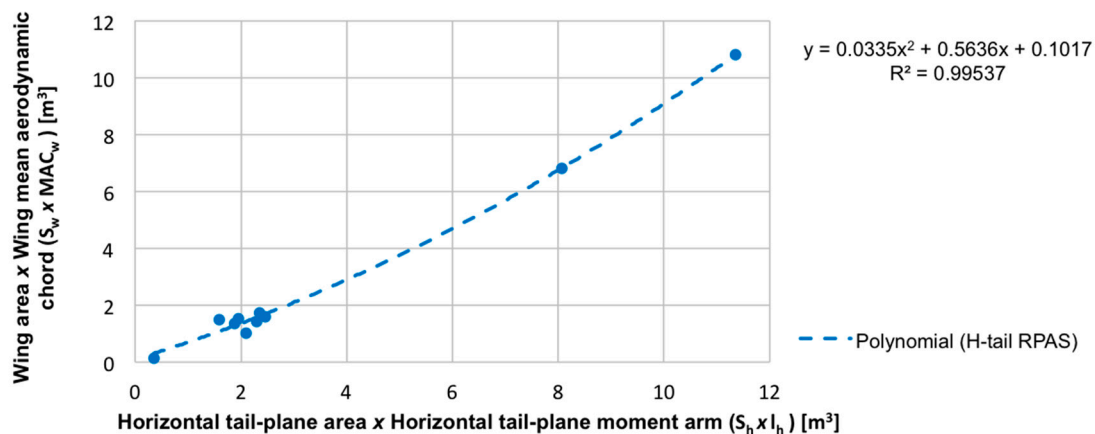

$$y = 0.0335x^2 + 0.5636x + 0.1017$$
$$R^2 = 0.99537$$

Figure 6. Wing area $\times$ Wing mean aerodynamic chord–Horizontal tail-plane area $\times$ Horizontal tail-plane moment arm correlation, with a typical error of 0.26 m^3.

A proposed method for obtaining the HTP span is the following: since in the case of this aerodynamic surface the structural criteria are predominant relative to the aerodynamic criteria, the Aspect Ratio of the HTP can be estimated in half of that of the wing [10]. The reason for this is that in this case, it is not as convenient to design it with a considerable value or AR in order to reduce induced drag, as the lift that this surface provides is appreciatively lower than that of the wing, and as such, the inducted drag is also significantly lower. Therefore, as the AR penalizes the structural behavior of the aerodynamic surface due to augmenting the bending moment, the proposed relation between AR_w and AR_h can be set. Having fixed the AR_h value, the span of the HTP can be obtained, and considering that the design of this aerodynamic surface for this particular RPAS category is rectangular, the chord of the HTP can be estimated through the ratio of S_h and b_h, and thus the sizing of the HTP is completed.

3.2.3. VTP Design

In the H-tail category of RPAS the position and design of the HTP and the VTP are geometrically related, since both are located at the end of the tail booms that usually extend from the wing, a geometric approach will be followed in some of the design phases of this aerodynamic surface, as the sizing of the HTP will have already determined some of the characteristics of the VTP. As noted in the second section of this paper, it should also be taken into account that the planforms of the vertical tail-planes of the aircraft in the database included in the H-tail category present a significant diversity of planforms, consisting in different trapezial sections of varying taper ratio and sweep angles. For this reason, the equivalent VTP was defined in the aforementioned section, thus pretending to reduce the scatter of the correlations which will be estimated.

A usual method for sizing S_v for twin-engine aircraft is to consider the engine failure scenario, in which the vertical tail-plane and rudder need to compensate for the moment created by the remaining engines. However, this is not the case in most RPAS, which have only a single engine. Therefore, another approach is considered, which consists in estimating a correlation between MTOW and S_v, which is represented in Figure 7.

Having estimated the value of S_v, the next proposed step in the design process would be to decide the relative vertical position between the HTP and the VTP. Among the aircraft included in the H-tail group, a significant variety is observed in the vertical position of the HTP along the twin-vertical tail-planes span. In most cases, the HTP is located at the bottom of the VTP span, or at approximately 15% of the span of the vertical tail-plane. However, in other RPAS, it is positioned at 50% of b_v, and the final tendency which has been observed is to locate it at the top of the VTP, as in the case of a T-tail with twin VTPs. As it will be seen in the following design steps, the relative position of both surfaces serves as a criterion to classify the aircraft in different groups, each of which will have typical values of AR_v and λ_v.
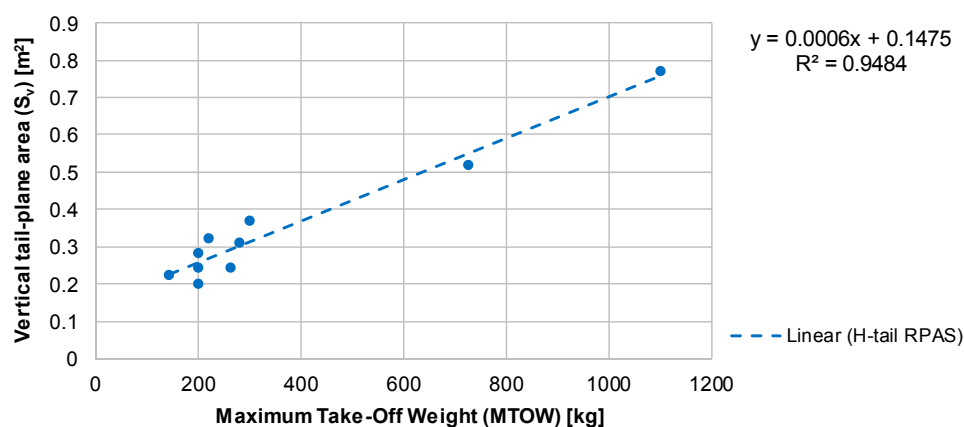

Figure 7. Vertical tail-plane area–Maximum Take-Off Weight correlation, with a typical error of 0.042 m^2.

Since the only design parameter of the VTP known is the surface, a further step is taken that will also contribute in deciding the relative vertical position between both surfaces, and that is estimating the moment arm (l_v). In the case of the VTP, as the moment arm of the HTP has already been defined and both surfaces are located at the end of the tail booms, it would be sensible to assume that a geometric relation can be set between them. Therefore, the correlation represented in Figure 8 is estimated, which compares both moment arms, l_h and l_v. Entering the correlation with the value of l_h, the VTP moment arm can be obtained. With this value, the volume coefficient of the vertical tail (V_v) can also be estimated, since the required data which define this dimensionless parameter have already been obtained: S_v, S_w, and b_w.

$y = 1.1073x - 0.217$
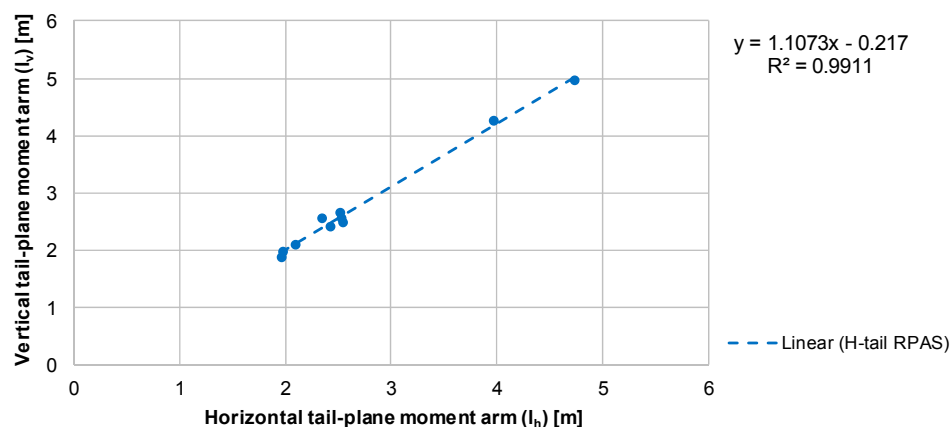$R^2 = 0.9911$

– – – Linear (H-tail RPAS)

Figure 8. Vertical tail-plane moment arm–Horizontal tail-plane moment arm correlation, with a typical error of 0.10 m.

Having obtained the value of l_v, the next step would be to determine the relative vertical position of the VTP and HTP. This decision will consequently lead to a categorization of the aircraft into diverse groups, similar to that which was proposed in the case of the wing, and which will aid in determining the value of the Aspect Ratio and taper ratio of the VTP. It can be observed that most of the aircraft opt for an HTP position at the bottom of the VTP or at approximately 15% of its span. This is probably due to the benefits of having the horizontal tail-plane in the slipstream of the propeller, as was also commented in Section 3.1 when addressing the different design tendencies of RPAS, since the dynamic pressure is higher and thus larger aerodynamic forces can be obtained with the same HTP surface. However, as noted in previous studies [26], this increase in dynamic pressure drops rapidly as the horizontal tail-plane is moved upward along the vertical tail, exiting the region where the highest increase in dynamic pressure occurs. Therefore, it is expected that, while the previously commented positions of the HTP allows for the designer to benefit from this phenomenon, upon moving the HTP upward along b_v, this effect can no longer be achieved. The reasons why an upper position for the HTP are selected can be diverse, and are most probably dependent on the configuration of the fuselage, the propeller slipstream or specific criteria related to the mission. The disposition of locating the HTP at the top of the vertical tail-planes is similar to that of T-tail airplanes, and thus it can be assumed that the aerodynamic, structural, and aeroelastic disadvantages that were previously commented upon in Section 3.1 when describing the T-tail configuration are also present in this case. This may explain why, save for particular cases in which other factors make this configuration preferable, it is less often used than the aforementioned one. The last scenario consists in locating the HTP approximately at 50% of the vertical tail span, which constitutes a middle ground between the other cases.

When the vertical position of the HTP is selected, another parameter of the VTP can be fixed, and that would be the chord at the union with the HTP, which will be set to the equal to the chord of the HTP. This consideration, which is also geometric, is consistent with the observed design of H-tail RPAS. In the case that the HTP is to be located at the bottom of the VTP, the root chord of the VTP (cr_v)

would be set to be the same as the chord of the horizontal tail-plane which was estimated in earlier steps of the design process. Should the HTP be at the top of the VTP, then it would be the tip chord (ct_v) the parameter that would be fixed.

In order to establish an organized criterion for this step in the design process, the flowchart represented in Figure 9 allows us to categorize the design aircraft in a similar way to the process that was followed in the wing design. This will allow us to define typical values of AR_v and λ_v which will allow for obtaining more precise results in the design of the VTP. The criteria which will be used in this classification will consider the following aspects: relative position of the HTP and VTP according to the criteria exposed earlier in this section, expressed as the percentage of b_v at which the HTP is located, moment arm of the VTP (l_v), and MTOW.
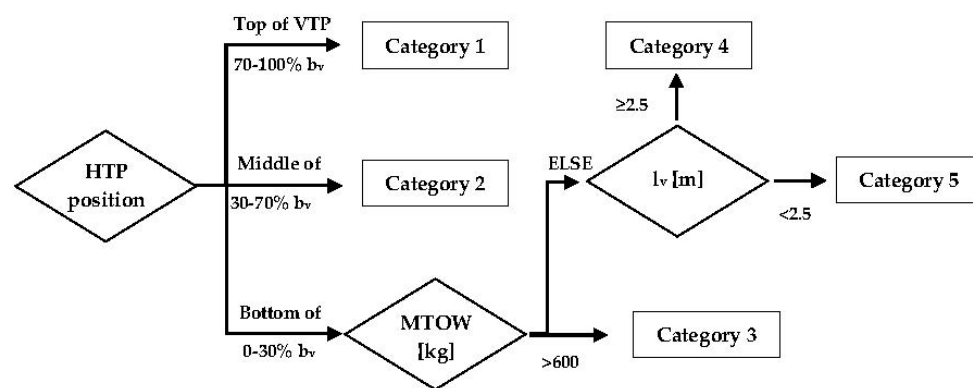

Figure 9. Flowchart for the categorization of RPAS in groups of similar vertical tail-plane (VTP) taper.

The first classification criteria (location of HTP) will also determine the chord of the VTP at the designated position. Further criteria allows to group aircraft with similar VTP planforms so as to select a value of λ_v amongst a category of aircraft with less scatter than the global sample. Table 5 provides an insight on various design parameters related to the tail which allows the designer to visualize the characteristics of the tail design close to its finalization.

Table 5. RPAS classification attending to tail design.

Category	Typical VTP Position (%b_v)	AR_v (-)	l_v (m)	Λ_{vle} [1] (°)	λ_v Range	λ_v Mean
1	100	(1.30–1.60)	(1.90–2.50)	(0–20)	(0.55–0.80)	0.67
2	(40–60)	(1.60–2.30)	(1.80–2.10)	(10–35)	(0.40–0.55)	0.47
3	(15–20)	(1.60–2.10)	(4.00–5.00)	(0–30)	(0.50–0.70)	0.59
4	(0–30)	(1.70–2.00)	(2.50–3.00)	(5–40)	(0.30–0.40)	0.32
5	0	(2.00–2.30)	(2.10–2.50)	0	1	1

[1] Λ_{vle} represents the leading-edge sweep angle of the VTP.

The parameters that are shown in Table 5 can also aid in explaining the reason for the typical values of taper that can be observed in each group. As in the wing design section, the taper ratio alleviates the structural loads experienced by the aerodynamic surface, since it reduces the bending moment that in this case is transferred by the tail booms to the strengthened structure. The parameter AR_v has been selected for this comparison since it provides an idea of the span of the VTP compared to its surface, which can directly relate to the aforementioned structural criteria, since a large Aspect Ratio provides worse structural behavior precisely due to the larger bending moments. The parameter l_v was also chosen because the structural loads suffered in the tail must be transferred to the wing. Therefore, large values of l_v will also penalize the structural behavior. Finally, the value of the leading-edge sweep angle (Λ_{vle}) was also selected because it also augments the bending moment suffered, in this

case, in the tail booms, and therefore lower values of λ_v should be selected in order to improve the structural behavior [10].

For the first category, in which the HTP is located at the top of the vertical tail-planes, lower values of AR_v compared to the other categories can be observed. This is precisely due to the comparatively worse structural behavior of a T-tail configuration, which is similar to the selected tail disposition in this category. Since the loads of the horizontal plane are transferred to the vertical tail-planes instead of being directly transferred to the tail booms, lower values of Aspect Ratio are selected in order to alleviate the stresses in the VTPs. Similarly, this can explain the values of the taper ratio, since a lower taper ratio, which results in a larger difference between ct_v and cr_v, contributes to the structural behavior of the aerodynamic surface. The reason for not selecting even lower taper ratios could be due to the HTP being located precisely at the top of the vertical tail-planes. Thus, if lower values would be selected, and as the tip chord of the VTP is fixed at the same value as the chord of the HTP, the root chord of the VTP could be larger than desired. In the case of the second category, which corresponds to a middle position of the HTP along b_v, the values of the different design parameters also fall in a middle ground amongst the ones that correspond to the other groups.

The last three categories correspond to a low position of the HTP. Category 3 groups the aircraft with larger values of MTOW, and thus also larger moment arms (l_v). It can be checked that lower values of λ_v are selected, which is probably motivated by the higher aerodynamic loads to be expected in these aircraft, the high values of l_v and possibly moderate values of Λ_{vle}, all of which contribute to augmenting the bending moments transferred to the wing structure. In the case of category 4, the lower values of taper ratio can be observed, even though the HTP is located in a low position. This is probably due to the large values of l_v and Λ_{vle} when compared to other aircraft in their MTOW range, which is much lower than those included in category 3. Therefore, the taper ratio of the VTP has to be lowered so as to not penalize excessively the structural behavior. Finally, category 5 corresponds to the particular case of rectangular VTPs, which are not structurally as advantageous as tapered VTPs but may be selected due to not presenting sweep angle and in the case that the aerodynamic loads in the tail are not expected to be significant enough to modify the value of these parameters.

Having fixed the value of the VTP chord at the station of the HTP and the taper ratio (λ_v) according to the categorization proposed beforehand, and having obtained the value of S_v earlier in the design process, the values of b_v, cr_v, or ct_v depending on the case, and finally MAC_v can be obtained by solving the equation system (5–7) that was defined in the wing design section, albeit entering the equations with the parameters of the VTP. As the values of S_v, l_v are known, employing the wing surface (S_w) and wingspan (b_w) parameters, the value of the volume coefficient (V_v) can also be obtained through Equation (4). Finally, a value of the sweep angle can be selected observing the information in Table 5 in order to finalize the design of the VTP.

3.3. Design Example Case

In order to test the accuracy of the proposed design method for the category of H-tail RPAS, a design case is proposed. An aircraft that has not been included in the database will be examined and designed starting from the design specifications that were at the first step of the design process. Since in the correlations, as has been noted beforehand, many of the studied aircraft are included in the range of MTOW between 100 kg and 300 kg, whereas two other aircraft have significantly larger values of MTOW, it has been decided to select as the sample aircraft one that is in the most representative range so as to assure the veracity of the results.

The aircraft chosen to develop the design case is the RQ-2 Pioneer, an aircraft developed jointly by AAI Corporation (Hunt Valley, MD, US) and IAI (Lod, Israel), with an H-tail configuration and equipped with a piston engine and a two-blade pusher propeller designed for surveillance missions. The design specifications of this aircraft, which serve as the input for the design procedure, are the following: the MTOW (205 kg), the value of endurance provided by the manufacturer (5 h), and the typical cruise speed (200 km/h). These input data are presented schematically in Table 6.

Table 6. Design example case input data.

Input Parameter	Units	Value
MTOW	kg	205
E	h	5
V_c	km/h	200

For every step of the design process, the value obtained following the design procedure and the relative error percentages, shown between parentheses, according to the actual values are expressed. Tables 7–9 summarize the results of the design process, providing the comparison between the real values and the ones obtained following the proposed rapid-sizing method. It has been checked that the predicted point falls within the margin provided by the typical error of each correlation.

Table 7. Design example case results for the wing design.

Parameter	Units	Real Value	Estimated Value	Relative Error (%)
S_w	m^2	3.18	3.23	−1.63
b_w	m	5.13	5.40	−5.19
λ_w	-	1.00	0.97	+3.00
cr_w	m	0.62	0.61	+1.91
ct_w	m	0.62	0.59	+4.85
MAC_w	m	0.62	0.60	+3.38

Table 8. Design example case results for the horizontal tail-plane (HTP) design.

Parameter	Units	Real Value	Estimated Value	Relative Error (%)
S_h	m^2	0.59	0.60	−1.25
l_h	m	2.200	2.205	−0.29
V_h	-	0.66	0.68	−3.41
λ_h	-	1	1	0
b_h	m	1.79	1.64	+8.30
cr_h	m	0.33	0.36	−10.42
ct_h	m	0.33	0.36	−10.42
MAC_h	m	0.33	0.36	−10.42

Table 9. Design example case results for the VTP design.

Parameter	Units	Real Value	Estimated Value	Relative Error (%)
S_v	m^2	0.25	0.27	−10.30
l_v	m	2.20	2.22	−1.22
V_v	-	0.033	0.034	−4.42
λ_v	-	1	1	0
cr_v	m	0.33	0.36	−11.44
ct_v	m	0.33	0.36	−11.44
MAC_v	m	0.33	0.36	−11.44
b_v	m	0.75	0.74	+1.02

Observing the proposed design process steps and the error committed compared to the geometric data of the aircraft provided by the manufacturer and the typical error of these correlations, it can be concluded that the method could be considered an acceptable approach in providing a rapid-sizing of the RPAS adequate to the first steps in the design process. In this conceptual design phase, the focus is set on obtaining a first approach to the geometry and characteristics of the aircraft, employing rapid methods so as to define the layout of the RPAS and take the fundamental design decisions. In further

steps of the design process, it would be expected that employing more complex and detailed methods, the error is reduced, and the design becomes more refined.

4. Conclusions

The focus of this work has been in addressing the study of conceptual design methods for Remotely Piloted Aircraft Systems (RPAS), both in terms of studying the diverse design tendencies of fixed-wing RPAS, so as to understand the different design decisions relative to aerodynamic configuration and power plant that must be taken in the first steps of the design process, and with the purpose of investigating the development of rapid-sizing methods for the conceptual design phases of these aircraft. The current context of the RPAS industry can explain the need for such a methodology, since the dynamism of the sector calls for the use of rapid-sizing methods that can aid manufacturers to achieve a favorable position in the market. Furthermore, previous aircraft design methods do not take into account the particularities of these aircraft, such as the feasibility of lower values of MTOW, so the development of a tool intended specifically for these aircraft can also be considered one of the main contributions of this manuscript.

With this objective, an extensive database of RPAS has been developed, from which a study of diverse categorizations has yielded a series of conclusions relative to the aforementioned design tendencies. Regarding this subject, is has been deduced that some specific configurations, concretely the ones of conventional tail, T-tail, V-tail, H-tail, and tailless, dominate the majority of RPAS designs currently in the market. Other aerodynamic configurations have also been employed. However, they have not yet reached the degree of expansion which the aforementioned ones have obtained. Different conclusions regarding the use of these configurations relative to the aircraft Maximum Take-Off Weight (MTOW) and the equipped power plant have been deduced. Therefore, it can be concluded that these three categorizations (aerodynamic configuration, MTOW, and power plant) are clearly associated, and that depending on the mission of the aircraft and the various design requisites established, a conjunction of these three characteristics can be selected in order to establish the basis of the aircraft design.

Furthermore, for one of the aerodynamic configurations which were studied, the H-tail layout, sufficient data were available so as to undertake the development of a rapid-sizing method based on statistical correlations obtained from the information on different parameters included in the database. It was observed that several accurate correlations relative to geometric parameters such as the surfaces of the wing (S_w) and tail-planes (S_h, S_v) and others based on definitions of dimensionless parameters such as the volume coefficients (V_h, V_v) could be obtained. Other methods, such as the categorization of aircraft attending to performance and geometric parameters were also proposed, so as to estimate the values of certain parameters such as the taper ratios (λ_w, λ_v) through observation of the values of these parameters in similar RPAS. The proposed method allows for a rapid sizing of the wing and the tail-planes. This allows us to deduce that a method based on statistical regressions similar to those proposed by other authors for different aircraft types can also be developed for RPAS, obtaining reasonably accurate correlations and conclusions that are coherent with different structural and aerodynamic design criteria.

Finally, in order to check the viability of the proposed design method, it has been applied to a design scenario, selecting the H-tail aircraft RQ-2 Pioneer, for which the geometric data were known. Comparing the results obtained through the design process with the data provided by the manufacturer, it can be concluded that the accuracy of the rapid-sizing method can be considered acceptable in the conceptual design phase of an RPAS project, since the errors obtained in the estimation of the different geometric parameters are according to the typical errors committed in this stage. Therefore, the aforementioned methods based on statistical correlations can be applicable as rapid-sizing tools for the conceptual design of RPAS.

References

1. Cuerno-Rejado, C.; García-Hernández, L.; Sánchez-Carmona, A.; Carrio, A.; Sánchez-Lopez, J.L.; Campoy, P. Evolution of the unmanned aerial vehicles until present. *DYNA* **2015**, *90*, 281–288. [CrossRef]

2. Fahlstrom, P.G.; Gleason, T.J. *Introduction to UAV Systems*, 4th ed.; Wiley: Chichester, UK, 2012; ISBN 978-1-119-97866-4.

3. European Comission. Flying New Way RPAS. 2016. Available online: http://ec.europa.eu/DocsRoom/documents/19184 (accessed on 26 October 2017).

4. Austin, R. *Unmanned Aircraft Systems: UAVS Design, Development and Deployment*; Wiley: Chichester, UK, 2010; ISBN 978-0-470-05819-0.

5. Barnhart, R.K.; Hottman, S.B.; Marshall, D.M.; Shappee, E. (Eds.) *Introduction to Unmanned Aircraft Systems*; CRC Press: Boca Raton, FL, USA, 2012; ISBN 978-1-439-83520-3.

6. Office of the Secretary of Defense, Department of Defense. *Unmanned Systems Roadmap 2005–2030*; Office of the Secretary of Defense: Arlington, VA, USA, 2005.

7. Federal Aviation Administration. *FAA Aerospace Forecast Fiscal Years 2017–2037*; Federal Aviation Administration: Washington, DC, USA, 2017.

8. ICAO. *Circular 328, Unmanned Aircraft Systems (UAS)*; ICAO: Montréal, QC, Canada, 2011.

9. ICAO. *Remotely Piloted Aircraft Systems Symposium*; ICAO: Montréal, QC, Canada, 2015; Available online: https://www.icao.int/Meetings/RPAS/Pages/RPAS-Symposium-Presentation.aspx (accessed on 27 October 2017).

10. Torenbeek, E. *Synthesis of Subsonic Airplane Design*; Springer: Dordrecht, The Netherlands, 1982; ISBN 978-90-481-8273-2.

11. Roskam, J. *Airplane Design*; DAR Corporation: Lawrence, KS, USA, 1985; Volume I–VIII, ISBN 978-9-993-24960-3.

12. Raymer, P.D. *Aircraft Design: A Conceptual Approach*; AIAA Education Series: Sylmar, CA, USA, 2012; ISBN 978-1-600-86911-2.

13. Kallinderis, Y.; Vouvakos, X.; Menounou, P. Linear correlations of principal parameters for the preliminary design of twin civil jet aircraft. *Aircr. Eng. Aerosp. Technol.* **2009**, *81*, 508–515. [CrossRef]

14. Vouvakos, X.; Kallinderis, Y.; Menounou, P. Preliminary design correlations for twin civil turboprops and comparison with jet aircraft. *Aircr. Eng. Aerosp. Technol.* **2010**, *82*, 126–133. [CrossRef]

15. Nicolai, L.; Carichner, G. Aircraft design. In *Fundamentals of Aircraft and Airship Design*; Schetz, J.A., Ed.; AIAA Education Series: Blacksburg, VA, USA, 2010; Volume I, ISBN 978-1-600-86751-4.

16. Cuerno-Rejado, C.; Sánchez-Carmona, A. Preliminary sizing correlations for the rear-end of transport aircraft. *Aircr. Eng. Aerosp. Technol. Int. J.* **2016**, *88*, 24–32. [CrossRef]

17. Sóbester, A.; Keane, A.J.; Scanlan, J.; Bressloff, N.W. Conceptual design of UAV airframes using a generic geometry service. In Proceedings of the Infotech@Aerospace Conferences, Arlington, VA, USA, 26–29 September 2005; AIAA 2005-7079. American Institute of Aeronautics and Astronautics: Reston, VA, USA, 2005. [CrossRef]

18. Beaman Howe, W. Design Methods for Remotely Powered Unmanned Aerial Vehicles. Master Thesis, Faculty of California Polytechnic State University, San Luis Obispo, CA, USA, 2015. [CrossRef]

19. Harmon, F.G.; Frank, A.A.; Chattot, J.-J. Conceptual design and simulation of a small hybrid-electric unmanned aerial vehicle. *J. Aircr.* **2006**, *43*, 1490–1498. [CrossRef]

20. Jay, G. *Designing Unmanned Aircraft Systems: A Comprehensive Approach*; AIAA Educational Series: Reston, VA, USA, 2013; ISBN 978-1-600-86843-6.

21. Kottakota, I. Selecting principal parameters of baseline design configuration for twin turboprop transport aircraft. In Proceedings of the 22nd Applied Aerodynamics Conference and Exhibit, Providence, RI, USA, 16–19 August 2004; AIAA 2004-5069. American Institute of Aeronautics and Astronautics: Reston, VA, USA, 2005. [CrossRef]

22. Watts, A.C.; Ambrosia, V.G.; Hinkley, E.A. Unmanned aircraft systems in remote sensing and scientific research: Classification and considerations of use. *Remote Sens.* **2012**, *4*, 1671–1692. [CrossRef]

23. Federal Aviation Administration. *Part 107—Small Unmanned Aircraft Systems*; Federal Aviation Administration: Washington, DC, USA, 2016.

24. European Aviation Safety Agency. *NPA 2017-05 Introduction of a Regulatory Framework for the Operation of Drones*; European Aviation Safety Agency: Cologne, Germany, 2017.

25. Valavanis, K.P.; Vachtsevanos, G.J. (Eds.) *Handbook of Unmanned Aerial Vehicles*; Springer: Dordrecht, The Netherlands, 2015; ISBN 978-90-481-9706-4.

26. Sweberg, H.H. *The Effect of Propeller Operation on the Air Flow in the Region of the Tail Plane for a Twin-Engine Tractor Monoplane*; NACA Report, N 62 65381; NACA: Washington, DC, USA, 1942.

27. Torenbeek, E. *Advanced Aircraft Design: Conceptual Design, Analysis and Optimization of Subsonic Civil Airplanes*; Wiley: Chichester, UK, 2013; ISBN 978-1-118-56811-8.